Accurate 12D dipole moment surfaces of ethylene

Thibault Delahaye, Andrei Nikitin, Michael Rey, Peter G. Szalay, Vladimir G. Tyuterev

Accurate 12D dipole moment surfaces of ethylene

Thibault Delahaye[a,*], Andrei V. Nikitin[b,c], Michael Rey[a], Péter G. Szalay[d], Vladimir G. Tyuterev[a]

[a] *Groupe de Spectroscopie Moléculaire et Atmosphérique, UMR CNRS 7331, BP 1039, F-51687, Reims Cedex 2, France*
[b] *Laboratory of Theoretical Spectroscopy, Institute of Atmospheric Optics, Russian Academy of Sciences, 634055 Tomsk, Russia*
[c] *QUAMER, State University of Tomsk, Russia*
[d] *Institute of Chemistry, Eötvös Loránd University, P.O. Box 32, H-1518 Budapest, Hungary*

Abstract

Accurate *ab initio* full-dimensional dipole moment surfaces of ethylene are computed at 82 542 nuclear configurations using coupled-cluster approach and its explicitly correlated counterpart CCSD(T)-F12 combined respectively with cc-pVQZ and cc-pVTZ-F12 basis sets. Their analytical representations are provided through 4-th order normal mode expansions. First-principles predictions of line intensities in rotationally resolved spectra using variational method up to $J = 30$ are in excellent agreement with experimental data in the range 0-3200 cm^{-1}. Errors of 0.25 - 6.75% in integrated intensities for fundamental bands are comparable with experimental uncertainties. Overall calculated C_2H_4 opacity in 600-3300 cm^{-1} range agrees with experimental determination better than to 0.5%. The improved accuracy permitted to resolve some controversial issues related to the qualitative behavior of intensity patterns.

☆DOI: 10.1016/j.cplett.2015.09.042.
*Corresponding author
Email addresses: `thibault.delahaye@lisa.u-pec.fr.fr` (Thibault Delahaye), `michael.rey@univ-reims.fr` (Michael Rey)

1. Introduction

Radiative properties of hydrocarbons, including the ethylene (ethene) C_2H_4 molecule, are of major importance in various domains of science particularly for remote gas sensing applications [1]. In the Earth atmosphere ethylene is a natural gas pollutant [2, 3, 4] produced by various sources as forest fires, volcanic eruptions, combustion processes and also by anthropogenic emissions due to motor vehicle exhaust. It is involved in bio-chemical processes acting as a hormone in plant biology regulating growth and development and is used for fruit ripening control [5].

Together with other simple hydrocarbons ethylene is one of key molecules for various astrophysical applications [6, 7]. They dominate the opacity of some brown dwarfs and asymptotic-giant-branch (AGB) stars and are considered among "standard" building blocks for carbon-rich atmospheres of many exoplanets [7]. Spectral signatures of ethylene have been observed in the outer planets Jupiter, Saturn, Neptune, and satellites [6].

Accurate knowledge of line and band intensities as well as of their temperature dependence is essential for reliable remote sensing diagnostics. Rotationally resolved ethylene spectra are known to be quite complex due to irregular couplings of twelve vibrational modes. Their analyzes represent difficult tasks because of accidental resonance perturbations in congested patterns of overlapping bands including hot ones. For this reason the ethylene line-by-line information in available spectroscopic databases [8, 9] is far from being complete.

Ab initio theoretical studies of triatomics and small polyatomic molecules of planetological and astrophysical interest such as ammonia NH_3, phosphine PH_3, methane CH_4 grew up during last decades along with the improvement of *ab initio* surfaces and computational codes solving the rovibrational Schrödinger equation (see for example Refs. 10, 11, 12, 13, 14, 15, 16, 17, 18, 19 and references therein). This has helped resolving many issues related to spectra analyzes at high energy ranges [20, 21, 14, 22, 23] (the list being not exhaustive). Quantitatively accurate *ab initio* rovibrational spectra of five-atomic

hydrocarbon isotopologues have been recently reported [16, 24, 25] together with detailed comparison against experimental data. Examples of global high-temperature methane spectra predictions for astrophysical applications can be found in Refs. 26, 27. Concerning the ethylene molecule, data assignments and analyzes present in databases remain much more sparse, although many recent studies [28, 29, 30, 31, 32, 33] tend to extend the informations. For these reasons it is a perfect candidate to take the next step in accurate *ab initio* spectra calculations.

Accurate dipole moment surfaces (DMS) are mandatory for first principles intensity predictions [10, 11, 14, 34, 15, 35, 16, 19]. This requires high-level electronic structure calculations on an extended grid of points, an appropriate modeling of full-dimensional surfaces and converged nuclear motion variational calculations. These tasks become very demanding with increasing number of vibrational degrees of freedom and represent a considerable challenge for the theory in case of rotationally resolved spectra of six-atomics. This may explain a lack of related studies for the ethylene molecule at the theoretical level similar to that of three-to-five atomic molecules. Despite of promising accuracy of *ab initio* calculations for ethylene energy levels [36, 37, 38] and line intensities [34], there exist very limited public available information on the ethylene DMSs.

This works aims at filling this gap. We provide analytical symmetry-adapted representation of full 12-dimensional (12D) ethylene DMSs computed at large extent of nuclear configurations (82 542 points) using the coupled-cluster approach CCSD(T) and its explicitly correlated counterpart CCSD(T)-F12 combined with cc-pVQZ and cc-pVTZ-F12 basis sets. The comparison with experimental spectra suggests that the corresponding first principle intensity calculations are currently the most accurate ones.

This Letter is structured as follows. Section 2 describes computational approach to the construction of *ab initio* DMSs together with a brief review of the previous works. Sections 3 and 4 are devoted to the variational method of intensity calculations in the normal mode representation and to the comparison of intensities in the 0-3200 cm^{-1} range with recent calculations, experimental

spectra and databases. The summary and conclusions are given in Section 5.

2. Electronic structure calculations

Force field constants of C_2H_4 have been calculated by Martin *et al.* [36] at a CCSD(T)/cc-pVTZ level. Avila and Carrington [37] have modified this field using Morse representation of the potential energy surface (PES) and computed vibrational energies of up to 4200 cm^{-1}. In our previous work the ethylene PES [38] have been computed on the grid of 82 542 nuclear configurations. The analytical PES modeling using sixth order expansion in curvilinear symmetry adapted coordinates involving about 2650 parameters [38] have permitted a considerable improvement of rovibrational energy predictions for several isotopologues.

Carter, Sharma and Bowman [34] computed ethylene DMS at the MP2/cc-pVTZ level of the theory over 22 219 nuclear configurations and reported line intensities in the range below 3200 cm^{-1}. To our knowledge these were the only *ab initio* intensities reported for ethylene. Although their study was encouraging with a good agreement for the fundamental bands [34] giving a typical accuracy of ∼10-20% , the corresponding DMSs have not been published.

In this work we compute new DMSs with larger electronic basis set at extended grid of points. For this purpose, we applied coupled cluster approach including single and double excitations [39] with the perturbative treatment of triple excitations, usually denoted as CCSD(T) method [40] that has proven its efficiency for high-resolution spectroscopy applications in recent years (see 18, 19 and references therein).

Calculations were carried out using well established Dunning's correlation consistent basis sets cc-pVQZ [41]. In addition, explicitly correlated calculations, which are expected to improve the basis set convergence of CCSD correlation energies, were considered for comparison purpose. A second set of DMS surfaces was calculated at the CCSD(T)-F12 level of the theory combined with specially optimized correlation consistent F12 basis set cc-pVTZ-F12 [42]. As

generally advised, CCSD(T)-F12a method was employed with this VTZ-F12 basis set. The MOLPRO program package version 2010.1 [43] was used to carry out all the *ab initio* calculations of electronic ground state energies. Dipole moments were computed as the derivative of the energy with respect to the weak external uniform electric field using the finite difference scheme with the field variation of ± 0.001 a.u. around at the zero field strength. The dependence of the dipole moments on the size of finite steps external field derivatives was not significant in the range of 0.002 - 0.0001 a.u. We have checked this for various nuclear configurations with three field variation steps: 0.0001, 0.001 and 0.002 a.u. This gave relative differences in the determined dipole moment values of the order of 10^{-5} or 10^{-4}.

Most of the calculations were done using the regional "Romeo" multiprocessor computer (Reims), "IDRIS" computer center of CNRS in Orsay and "JADE" cluster at CINES computer center in Montpellier. As a first step for the DMS construction, the dipole moment values in the electronic ground state were calculated with cc-pVQZ basis set on a grid of the 82 542 nuclear configurations described in Ref. 38. The distribution of the density of the DMS geometrical configurations which corresponds to the same grid choice as for our PES has been given in Fig. 1 of Ref. 38, with a maximum number of configurations near 5000-7000 cm^{-1} but a significant number of points extends up to 12 000-13 000 cm^{-1}. The number of contracted functions was 178 for VTZ-F12 and 230 for VQZ bases. Full DMS calculations for these large basis sets were quite demanding in terms of computer resources. Altogether, these calculations took about 90 000 hours (CPU time) for VTZ-F12 basis and 180 000 hours for VQZ basis.

In this work, we used our best equilibrium geometry parameters values $r_{H_e} = 1.080565$ Å , $r_{C_e} = 1.330898$ Å, $\alpha_e = 121.40176$ Degrees [Table I of Ref. 38], obtained by an empirical optimization as described in Ref. 38]. As already pointed out in previous works, these parameters are of primary importance for accurate description of rotational spectra, and were fixed to the same value for all calculations involving different basis sets.

The DMS components μ_α in the molecular fixed Eckart frame were repre-

sented as power series of normal modes coordinates q_i

$$\mu_\alpha(q_1, q_2, \cdots, q_{12}) = \sum_n K_n \ {}^\alpha\mathbf{B}_n^p(q_k) \tag{1}$$

where $k \in \{1, 2, \cdots 12\}$ and

$${}^\alpha\mathbf{B}_n^p(q_k) = ({q^{p_1}_{1_{A_g}}} {q^{p_2}_{2_{A_g}}} {q^{p_3}_{3_{A_g}}} {q^{p_4}_{4_{A_u}}} {q^{p_5}_{5_{B_{2g}}}} {q^{p_6}_{6_{B_{2g}}}} {q^{p_7}_{7_{B_{2u}}}} {q^{p_8}_{8_{B_{3g}}}} {q^{p_9}_{9_{B_{3u}}}} {q^{p_{10}}_{10_{B_{3u}}}} {q^{p_{11}}_{11_{B_{1u}}}} {q^{p_{12}}_{12_{B_{1u}}}})^{\Gamma_\alpha} \tag{2}$$

with $\Gamma_\alpha \in B_{1u}, B_{2u}, B_{3u}$ for $\alpha = z, y, x$, $p = \sum_{m=1}^{12} p_m \in \{1, 2, \cdots 4\}$ and n is a string of low case indices in Eq. (2).

The shape of normal modes and the relation of rectilinear normal coordinate with Cartesian ones were defined on the PES [38] computed at the same level of the theory. The techniques of related transformations have been described in the previous work [16] (and references therein). We fitted K_n parameters of the DMS expansion (1) to our *ab initio* dipole moment values using the weight function that depends on energy E/hc expressed in cm^{-1}

$$w(E) = \frac{\tanh(-a(E - E_0) + b)}{1 + b}. \tag{3}$$

where $a = 0.0005$ cm, $b = 1.002002002$ and $E_0 = 9000\ \mathrm{cm}^{-1}$. With this weighting function, which has been originally employed by Schwenke and Partridge in Ref. 44 for the fit of methane PES, the weight of *ab initio* points decrease for electronic energies above the E_0 value.

In total $254 + 254 + 194$ parameters up to fourth order were statistically well determined in this fit on the entire grid of all 3×82542 *ab initio* points. The details of the fit as well as the number of parameters involved in the fit of each component μ_α are given in Table 1. Note that the number of *ab initio* geometries was considerably larger than the number of fitted DMS parameters. Figure 1 shows the VQZ DMS error distribution of the final fit. The fit errors (defined as *ab initio* dipole moment value minus the value of the analytical DMS representation) are quite small up to energies $\sim 9\ 000\ \mathrm{cm}^{-1}$. A larger scatter

Table 1: Statistics for the fit of *ab initio* points with analytical DMS representations for the two basis sets.

Component[a]	StDev[b] VQZ	W-StDev[c] VQZ	W-StDev[c] VTZ-F12	nb. param.[d]
$\mu_z(B_{1u})$	0.0002090	0.0001420	0.0001430	254
$\mu_y(B_{2u})$	0.0018375	0.0000910	0.0000938	254
$\mu_x(B_{3u})$	0.0003493	0.0000116	0.0000108	194

[a] Symmetries labeled with respect to I^r representation.
[b] Standard deviations between *ab initio* values and DMS analytical representation, in Debyes.
[c] Weighted standard deviations between *ab initio* values and DMS analytical representation, in Debyes.
[d] Number of parameters in analytical representation used for the surfaces fit.

of points above this range occurs because the weighting function (3) quickly de-emphasizes energies above this threshold [44]. In order to further improve the fit, it would be necessary to include some higher order terms in the DMS expansion (1). We plan to do this in a future work, but the fourth order should be sufficient to check the accuracy of the *ab initio* surfaces for the fundamental and low overtone and combination bands.

Both CCSD(T)/cc-pVQZ and CCSD(T)-F12a/cc-pVTZ-F12 *ab initio* DMSs fitted in normal modes coordinates up to fourth order are provided as the electronic Supplementary Materials of this work.

3. First principles variational intensity calculations: computational procedure

In order to check the accuracy of obtained DMSs we used these surfaces for rovibrational line intensities in the infrared. Rovibrational energies and wavefunctions were determined using our recent ethylene PES reported in Ref. 38, which is referred to as DNRST PES hereafter. As described in details in our previous works [16, 38, 19], the rovibrational model used in our homemade TENSOR code is based on the complete normal-mode nuclear Hamiltonian in Eckart frame [45]. Besides providing all necessary transformations for a systematic symmetry-

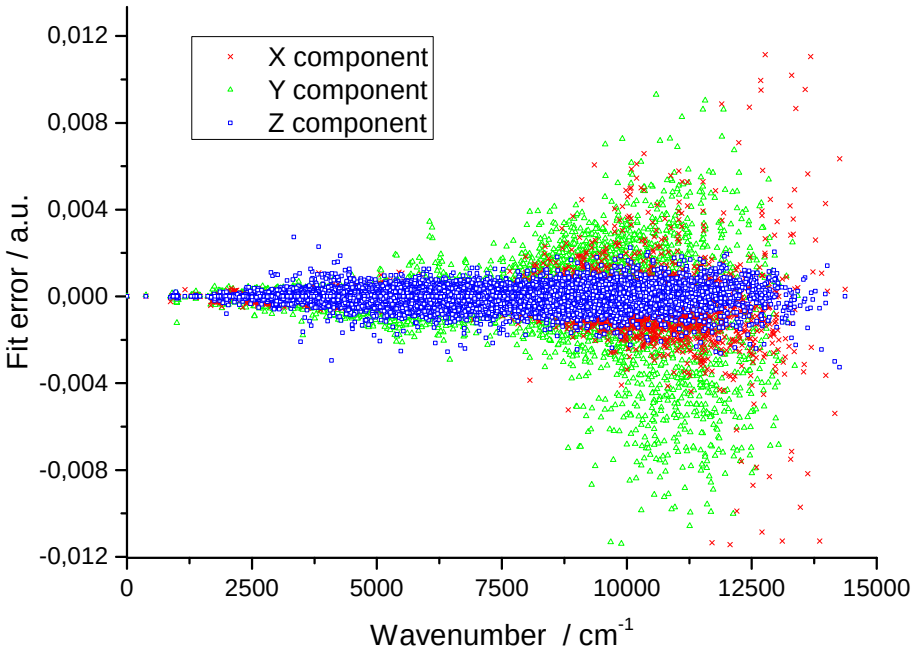

Figure 1: Errors of the ethylene DMS fit to *ab initio* values computed with the CCSD(T)/cc-pVQZ ansatz. Components x, y, z are represented in red, green and blue, respectively. (For interpretation of the references to color in this figure, the reader is referred to the web version of this article.)

adapted development of the complete normal-mode Hamiltonian expansion, this computational code implements variational procedure and reduction-truncation techniques for rovibrational spectra predictions. Following notations of Ref. 38, we used the six order reduced-truncated Hamiltonian $H_{10\to6}$, that is by retaining vibrational matrix elements up to $\Delta\mathbf{v}_{max} \leq 6$ in the 10-th order Taylor expansion. Convergence studies for the Hamiltonian expansions and for effects of the reduction procedure on vibrational levels, including the $H_{10\to6}$ model can be found in this latter work.

As described in details in previous works [16, 38], rovibrational line positions and intensities were obtained following a two steps procedure. First, band centers were calculated using *F(9)* basis of primitive normal mode vibrational functions satisfying the condition $F(\mathbf{v}_{max}) \Leftrightarrow \sum_i \kappa_i v_i \leq \mathbf{v}_{max}$. When available, vibrational $J = 0$ levels were matched to observed band centers[29, 33] using the

VSS empirical corrections [16, 38]. In order to make rovibrational calculations up to $J = 30$ feasible, we employed at the second step ($J > 0$) the eigenfunctions of vibrational Hamiltonian obtained at the first step according to the $F(9 \rightarrow r)$ basis compression scheme. Because of larger size of the resulting blocks for high values of the J quantum number, we limited the size of the reduced basis for *C-H* stretching modes by $F(9 \rightarrow 4)$ compression. For all other modes, we employed $r = 6$ for $0 \leq J \leq 10$ and $r = 5$ for $10 < J \leq 30$ compression schemes. With such basis size the rovibrational line positions would not yet be fully converged for high vibrational excitations. However, the previous work on phosphine and methane molecules has shown that this should not have a big impact on fundamental and low overtone and combination bands, particularly for integrated band intensities.

4. Comparisons of *ab initio* intensities with empirical values and with spectroscopic databases

An example of the comparison of predicted spectra using DNRST PES [38] and our *ab initio* DMSs with empirically based HITRAN line list of $^{12}C_2H_4$ for fundamental bands in the $600 - 3200$ cm^{-1} range is given in Figures 2, 3 and 4. Globally, all calculations with VQZ and VTZ-F12 basis sets are in a very good agreement with experimental intensities. In order to compare integrated intensities we extended line calculations up to rotational quantum number $J = 30$. In Tables 2, 3 and 4 integrated intensities in the ranges of fundamental bands are collected at 296 K and compared with various empirical data including HITRAN-2012 database, Lebron *et al.* [46], Bourgeois *et al.* [33] and with *ab initio* results of Carter *et al.* [34]. In all cases we use the HITRAN intensity units cm/molecule. Natural abundance factor 0.97729 of $^{12}C_2H_4$ was taken into account in all our calculated intensities.

First type of comparisons concerns rotationally resolved spectra. Figures 2, 3, 4 show a very good overall agreement of our line-by-line intensity calculations using *ab initio* VQZ and VTZ-F12 DMS with HITRAN spectroscopic database [8]

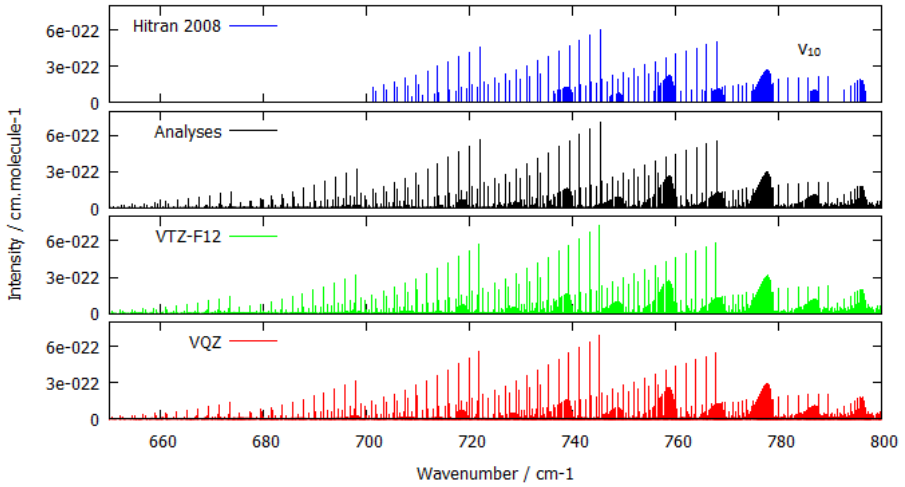

Figure 2: Comparison of spectra calculated from *ab initio* DMS using VQZ and VTZ-F12 basis sets with HITRAN 2012 and with latest experimental spectra analyzes[33] in 650 - 800 cm^{-1} region. In all calculations the DNRST PES [38] was used for line positions and vibration-rotation basis functions.

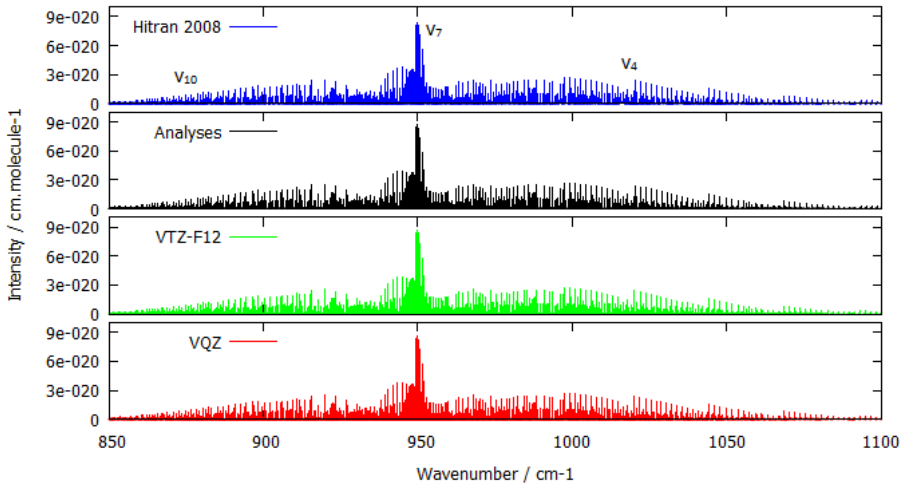

Figure 3: Comparison of spectra calculated from *ab initio* DMS using VQZ and VTZ-F12 basis sets with HITRAN 2012 and with latest experimental spectra analyzes[33] in 850 - 1100 cm^{-1} region. In all calculations the DNRST PES [38] was used for line positions and vibration-rotation basis functions.

and with the results of recent analyzes [33] of high-resolution experimental spectra in three ranges. Fig. 2 corresponds to the lowest edge of infrared active ethylene bands, Fig. 3 to ν_{10} wagging mode, ν_7 out-of-plane and ν_4 twisting vi-

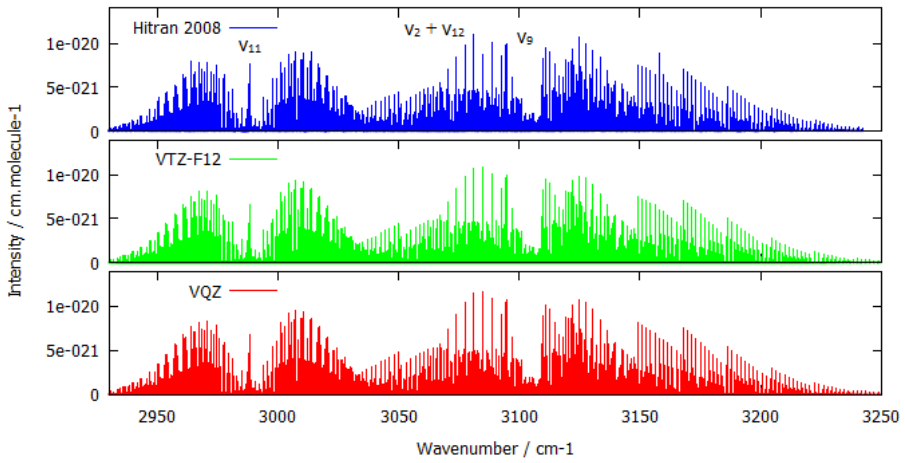

Figure 4: Comparison of spectra calculated from *ab initio* DMS using VQZ and VTZ-F12 basis sets with HITRAN 2012 in 2900 - 3250 cm^{-1} region. In all calculations the DNRST PES [38] was used for line positions and vibration-rotation basis functions.

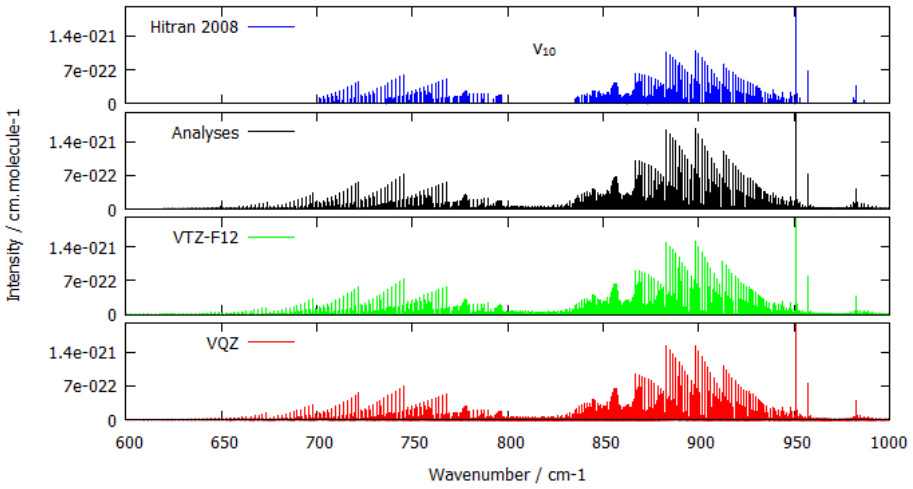

Figure 5: Comparison of the ν_{10} band of C_2H_4 calculated from *ab initio* DMS using VQZ and VTZ-F12 basis sets with HITRAN 2012 and with latest experimental spectra analyzes[33] in 600 - 1100 cm^{-1} region. In all calculations the DNRST PES [38] was used for line positions and vibration-rotation basis functions. It is clearly seen that HITRAN intensities were underestimated by about 30% with respect to new experimental analyzes and to our *ab initio* results.

brations whereas Fig. 4 corresponds to the range of higher frequency stretching fundamentals and some combination bands.

Figure 3 and 4 correspond to the ranges of the strongest ethylene absorbance.

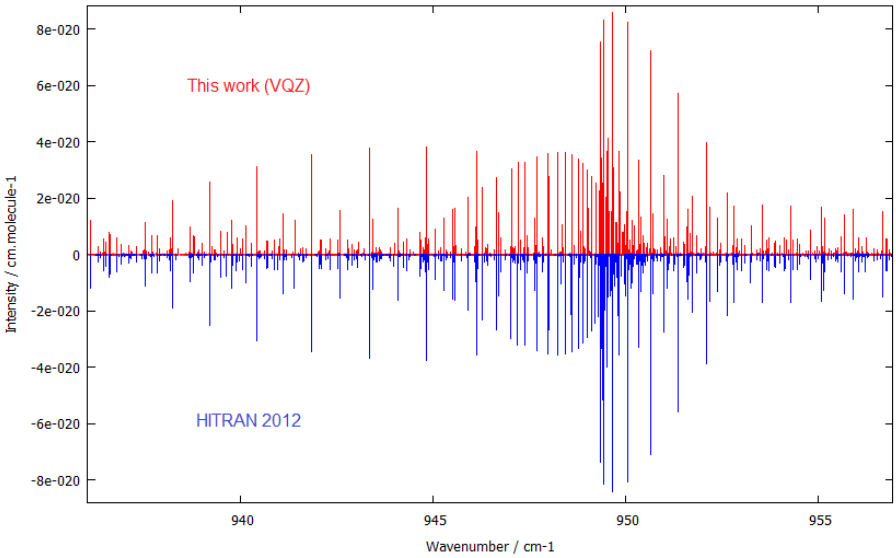

Figure 6: Comparison of spectra calculated from *ab initio* CCSD(T)/VQZ DMS with HITRAN 2012 in 935 - 958 cm^{-1} region. In our calculation the DNRST PES [38] was used for line positions and vibration-rotation basis functions. The VSS band center shift of -0.74 cm^{-1} was applied for ν_7.

On these scales both VQZ and VTZ-F12 DMSs give very similar band shapes. Due to better accuracy of our PES [38] and to the technique of VSS band center shifts [16] in two-step variational calculation, the deviations between calculated and observed line positions up to $J = 30$ appears to be of the order of 0.1 cm^{-1}. This allows better description of accidental rovibrational resonances than in previous theoretical studies. Figure 6 illustrates the line to line matching in the ν_{10}-ν_7 range.

Carter *et al.* [34] have reported good qualitative agreement for fundamental bands with some exceptions. They pointed out problems with the ν_{10} band in HITRAN suggesting mis-assignments. Here we confirm their finding concerning unsatisfactory representation of ν_{10} in HITRAN. Indeed the HITRAN intensities were too low and many of high-J transitions were missing in the center of the band and in the band edges that is clearly seen in Figures 2 and 5. However irregular strong lines (example at 951 cm^{-1}) appear here not because of mis-assignments but due to resonance intensity borrowing as further discussed in

Section 5. This conclusion is supported by recent results of new experimental spectra analyzes [33] which are in excellent agreement with our calculations (Figures 2 and 5).

Table 2 summarizes integrated intensities for six fundamental C_2H_4 bands for which the results of line-by-line high-resolutions spectra analyzes have been included in HITRAN database [8]. Integrated intensity in a range R is the sum $S = \sum_{i\ in\ R}^{S_i(min)} S_i$ of line intensities S for all calculated or observed transitions in this range. The cutoff $S_i(min) = 1.10^{-26}$ cm/molecule was applied for all bands. This accounts for the major part of the opacity at room temperature conditions. For known fundamental bands in case of VTZ-F12 DMS the deviations from empirical integrated intensity data (up to $J = 30$) range from 0.3% to 7%. The strongest ν_7 band deviates by 2.5% only. This is unprecedented accuracy of *ab initio* results for six-atomic molecules. Note that the RMS deviations in Table 2 and in further tables should not be entirely attributed to the errors in *ab initio* calculations as all available observed and empirical line lists used for the comparisons contain their own uncertainties which could amount to several percent as well. Another possible source of discrepancies is related to interference intensity effects among various bands, which are treated somewhat differently in experimental data reduction and in global theoretical predictions. For the total absorbance by six fundamentals accounting for 13 663 assigned rovibrational transitions (last line in Table 2) the difference with empirical data drops down to about 1%.

Second type of tests concerns interval-by-interval comparison of integrated intensities with low-resolution measurements (Table 3). Lebron and Tan [46] have reported Fourier transform experimental determination of the absorbance area in ethylene infrared spectra at a resolution of 0.5 cm^{-1} with various gas pressures. They have distinguished five spectral intervals given in Table 3 where the ethylene infrared opacity was the most significant.

The advantage of such comparison is that this implicitly involves contributions from line of all bands in the considered range including weak overtone, combination and hot bands which are not yet analyzed in high-resolution ex-

Table 2: Comparison of *ab initio* integrated intensities $\sum S_{is}$ for fundamental bands using VTZ-F12 and VQZ DMSs with empirical data deduced from high-resolution analyzes of rotationally resolved C_2H_4 spectra up to $J = 30$.

	$\sum S_{is}$				Diff.(%)[c]		RMS[d]
Band	VTZ-F12	VQZ	Empirical	Nb. trans.[b]	VTZ-F12	VQZ	pos.
ν_4	1.325×10^{-19}	1.313×10^{-19}	1.304×10^{-19}	461	-1.62	-0.66	0.056
ν_7	1.190×10^{-17}	1.187×10^{-17}	1.161×10^{-17}	3010	-2.50	-2.19	0.080
ν_{10}	3.497×10^{-19}	3.509×10^{-19}	3.674×10^{-19}[a]	4217	4.82	4.49	0.086
ν_{12}	1.364×10^{-18}	1.321×10^{-18}	1.463×10^{-18}	2378	6.75	9.69	0.062
ν_9	2.879×10^{-18}	3.097×10^{-18}	2.979×10^{-18}	2365	3.34	-3.98	0.131
ν_{11}	1.734×10^{-18}	1.752×10^{-18}	1.738×10^{-18}	1232	0.24	-0.80	0.160
Sum	1.836×10^{-17}	1.852×10^{-17}	1.829×10^{-17}	13663	-0.38	-1.26	0.070

Note: Intensities are in HITRAN units cm.molecule^{-1}, line positions RMS errors (last column) are in cm^{-1}. All "empirical" rovibrational lines assigned to known fundamental bands are taken from HITRAN-2012 database [8] except for ν_{10}.
[a]For ν_{10} empirical data are replaced by recent more accurate analysis [33].
[b]Number of lines used for the calculation of integrated band intensities.
[c]Relative deviations $[(S_{emp} - S_{calc})/S_{emp}]$ in % between empirical line lists and variational calculations using *ab initio* PES and DMSs.
[c]Deviations between empirical and calculated line positions up to $J = 30$.

Table 3: Interval-by-interval comparison of *ab initio* C_2H_4 integrated intensities with low resolution measurements of Lebron and Tan [46].

Ranges[a]	Principal bands[b]	Empirical [46][c]	This Work[d]	Diff.(%)[e]
$640 - 1200$	ν_7, ν_{10}, ν_4,...	1.33×10^{-17}	1.34×10^{-17}	0.75
$1340 - 1540$	ν_{12},...	1.66×10^{-18}	1.48×10^{-18}	10.84
$1820 - 1950$	$\nu_7 + \nu_8$,...	8.75×10^{-19}	7.27×10^{-19}	16.91
$1990 - 2100$	$\nu_6 + \nu_{10}$,...	1.04×10^{-19}	1.07×10^{-19}	-2.88
$2920 - 3260$	ν_9, ν_{11}, $2\nu_{10} + \nu_{12}$, $\nu_2 + \nu_{12}$	6.50×10^{-18}	6.76×10^{-18}	-4.00
Sum		2.24×10^{-17}	2.25×10^{-17}	-0.45

Intensities are in cm.molecule^{-1}.
[a]In wavenumbers $\left[\text{cm}^{-1}\right]$.
[b]Bands providing main contributions to considered interval.
[c]Measured by the total absorbance area in each interval [46].
[d]Obtained as a sum of VQZ *ab initio* line intensities for all bands contributing to each interval up to $J_{max} = 30$.
[e]Relative deviations $[(S_{obs} - S_{calc})/S_{obs}]$ in % between Ref. [46] and calculations for integrated line intensities.

Table 4: Summed up intensities of $J = 0, 1, 2$ ethylene transitions: comparison between *ab initio* predictions and HITRAN empirical data in the range of fundamental bands.

	$\sum S_{is}$			Discrepancies (%)[d]	
Range	Carter [34][a]	This Work[b]	Hitran[c]	Carter [34]	This Work
ν_7	1.26×10^{-19}	1.12×10^{-19}	1.14×10^{-19}	-12.46	-1.93
ν_{12}	1.47×10^{-20}	1.36×10^{-20}	1.37×10^{-20}	-7.89	-0.35
ν_9	2.24×10^{-20}	3.01×10^{-20}	3.07×10^{-20}	25.53	-2.24
ν_{11}	1.36×10^{-20}	1.61×10^{-20}	1.66×10^{-20}	15.13	-3.14
$2980 - 3125$[e]	3.97×10^{-20}	5.22×10^{-20}	5.18×10^{-20}	23.95	0.79

Note: Intensities are in cm.molecule^{-1}.
[a]$\sum S_{is}$ per band or per interval of all line intensities from Table V of Ref. 34.
[b]The same sample computed with our VQZ DMS.
[c]The same sample with empirical data from HITRAN-2012 database.
[d]Relative deviations $[(S_{emp} - S_{calc})/S_{emp}]$ in % between HITRAN and calculations.
[e]Wavenumber range in cm^{-1} including $\nu_2 + \nu_{12}$ and $2\nu_{10} + \nu_{12}$ combination bands.

periments. Also, this permits getting round very tedious line-by-line analyzes of rotationally resolved spectra and in a sense compensate incompleteness of HITRAN-like databases. For the comparison of Table 3 we have included between 2 and 10 times more theoretical lines than those presently available in HITRAN depending on the range. This gives an idea of a lack of information for ethylene data in existing databases. A shortcoming of the low resolution method is that it is locally less accurate and that contributions of impurities could hardly be totally excluded.

Bearing in mind above considerations, the agreement of our *ab initio* results with low-resolution Lebron and Tan measurements is also very good, particularly for the most absorbing regions 640 - 1200 cm^{-1} and 2920 - 3260 cm^{-1} were the deviations are of 0.75% and of 4%, respectively. In the middle ranges 1340 - 1540 cm^{-1} and 1820 - 1950 cm^{-1} the low resolution measurements show slightly larger absorption but could possibly be biased by a contribution of water vapor due to very large and strong ν_2 band centered at about 1600 cm^{-1}.

Finally we compared our intensities with previous *ab initio* results [34]. Carter *et al.* [34] have published large table including their calculated tran-

sitions for $J = 0, 1, 2$ for six bands ν_7, ν_8, ν_{11}, ν_{12}, $\nu_2+\nu_{12}$ and $2\nu_{10}+\nu_{12}$. They qualify their absolute intensities as quite acceptable. The agreement for strong bands was better than for the overtone bands where some lines were off up to 15-20 cm^{-1} in positions and up to factor 2-3 in intensities. In Table 4 we summarize these results by adding intensities of lines belonging to the same bands. This gives a sort of smoothing effect for outliers due to weaker lines. For the same reason the contributions at the highest range 2980 - 3125 cm^{-1} including two combination bands were summed up. With this averaging of $J = 0, 1, 2$ transitions the deviations of Carter *et al.* [34] from empirical data are in the range from 7% to 25% that can be considered as a good match for the first *ab initio* results. With our DMS the discrepancies for the same sample of data fall down to the range 0.4%-3% (Table 4).

5. Discussion and summary

After the pioneering work of Carter *et al.* [34], this study presents further improvement in theoretical predictions of ethylene intensities in the infrared. Few percent of Emp.-Calc. in Tables 2, 3, 4 are of the same order of magnitude as typical uncertainties of line intensity measurements and as errors in empirical models of experimental data reductions. In the Supplementary Electronic Materials we provide 12D *ab initio* DMSs that permit the accuracy of first principles intensity calculations comparable with available experimental precision. To our knowledge such a step forward in the computational spectroscopy becomes possible for the first time in case of rotationally resolved spectra of hexatomic molecules.

Also, the improved accuracy permitted resolving some controversial issues in qualitative intensity behavior. The first one concerns the intensity repartition between P and R branches depending on the band type. The P/R ratio for the strongest lines was not the same for certain bands in HITRAN and in the previous *ab initio* calculations [34]. For example, for the ν_{11} band the theoretical predictions of Ref. 34 gave weaker P-branch (P/R<1) in agreement

with HITRAN, whereas the opposite results occurred for the ν_{12} band: (P/R<1) in HITRAN and (P/R>1) in *ab initio* calculations [34]. In the present study the P/R ratios are in agreement with experimental data for all investigated bands. For example in the ν_{12} band we have the intensity ratio for the strongest lines $(P/R)_{\nu_{12}}^{ab\ initio} = 0.957$ that agrees well with the empirical ratio $(P/R)_{\nu_{12}}^{HITRAN} = 0.958$. The corresponding calculated transitions are $J, K_a, K_c = 10, 0, 10 \rightarrow 9, 0, 9$ at 1425.015 cm^{-1} in P-branch and $10, 0, 10 \rightarrow 11, 0, 11$ at 1461.701 cm^{-1} in R-branch. Note that the errors in our line position calculations for these transitions were only about 0.001 cm^{-1}.

The second controversy concerned irregular lines of the ν_{10} band. Carter *et al.* [34] attributed the most intense HITRAN line of ν_{10} at 951 cm^{-1} to an experimental mis-assignment as this did not appear in their calculated Fig.11 of ν_{10} [34]. By investigation of the wavefunction mixing coefficients we conclude that this is a case of so called "unstable transitions" [15, 22] whose intensities are known to be extremely sensitive to the accuracy of the PES and of the energy level calculations. In our calculations the upper state level $(J, K_a, K_c)_{\nu_{10}} = (18, 6, 12)$ at 1273.37 cm^{-1} of this transition is in accidental Coriolis resonance with the nearby level $(J, K_a, K_c)_{\nu_7} = (18, 2, 17)$ at 1273.60 cm^{-1}. A very small energy difference of only 0.23 cm^{-1} between these two upper state levels produces a strong resonance coupling between corresponding ν_{10} and ν_7 rovibrational states. In our calculations we have the normal mode decomposition for the wavefunction $\psi \ni V_{10}(70\%) + V_7(21\%) + ...$ of the first level. Consequently the line $J, K_a, K_c = 18, 1, 17 \rightarrow 18, 6, 12$ with the intensity $I = 3.71 \times 10^{-21}$ at 951.279 cm^{-1} has to be attributed to the ν_{10} band according to the major normal mode coefficient. This line appears as anomalously strong one due to the resonance intensity transfer from the line $J, K_a, K_c = 18, 1, 17 \rightarrow 18, 6, 12$ of ν_7 at 951.066 cm^{-1} that has the intensity $I = 1.19 \times 10^{-20}$. At this point we only partly confirm the statement of Carter *et al.* [34]: the effect of the intensity mixing with ν_7 indeed occurs but the first anomalously strong line at 951.279 cm^{-1} belongs to the ν_{10} band according to the wavefunction projection in agreement with HITRAN. The most recent new

experimental spectra analysis [33] in this range confirms our conclusion as seen in Figure 4. Note that in our calculation the position error is below 0.001 cm^{-1} for the first ν_{10} line and below 0.01 cm^{-1} for the second ν_7 line.

In higher energy ranges a correct description of "unstable lines" is a major challenge in computational spectroscopy both for first principle calculations and for assignment of crowded experimental spectra using effective polyad models [28, 30, 29, 31, 32]. In the first case small errors of few wavenumbers in energy levels would false the effects of "resonance intensity borrowing". On the other hand it is well known that the second types of methods suffer from ambiguity [47, 48, 49] of an empirical determination of the resonance coupling parameters responsible for these effects. One of possible solutions would be applying a mixed "*ab initio* $\rightarrow$ polyad model" approach, that permits characterizing various resonance couplings using *ab initio* information as was recently discussed for methane spectra [22].

This Letter was focused essentially on accurate DMS calculations and on the analytical surface model parametrization. More detailed comparisons with recent experimental data [31, 33] are planned in future works together with the study of nuclear basis convergence effects. Extended nuclear motion calculations using independent theoretical methods would help to produce accurate and sufficiently complete theoretical line lists in large infrared range for assignments and analyzes of experimental spectra.

6. Acknowledgments

The supports of the CNRS (France) and RFBR (Russia) in the frame of Laboratoire International Associé SAMIA , of Tomsk State University Academic D. Mendeleev funding Program, of IDRIS/CINES computer center of France and of the ROMEO computer center Reims Champagne-Ardenne are acknowledged.

Appendix A. Supplementary data

Supplementary data associated with this article can be found, in the online version, at http://www.sciencedirect.com/science/article/pii/S0009261415007319. Both CCSD(T)/cc-pVQZ and CCSD(T)-F12a/cc-pVTZ-F12 *ab initio* DMSs fitted in normal modes coordinates up to fourth order are provided.

References

[1] D. Weidmann, A. A. Kosterev, C. Roller, R. F. Ctoto, M. P. Fraser, F. K. Tittel, Appl. Opt. 43 (16) (2004) 3329–3334. doi:10.1364/AO.43.003329.

[2] S. Sawada, T. Totsuka, Atmos. Environ. 20 (5) (1986) 821 – 832. doi:http://dx.doi.org/10.1016/0004-6981(86)90266-0.

[3] J. H. Seinfeld, Science 243 (4892) (1989) 745–752. arXiv:http://www.sciencemag.org/content/243/4892/745.full.pdf, doi:10.1126/science.243.4892.745.

[4] C. P. Rinsland, C. Paton-Walsh, N. B. Jones, D. W. Griffith, A. Goldman, S. W. Wood, L. Chiou, A. Meier, J. Quant. Spectrosc. Radiat. Transfer 96 (2) (2005) 301 – 309. doi:http://dx.doi.org/10.1016/j.jqsrt.2005.03.003.

[5] F. Abeles, P. Morgan, M. Saltveit, Ethylene in Plant Biology, Elsevier Science, 1992.

[6] B. Bézard, J. I. Moses, J. Lacy, T. Greathouse, M. Richter, C. Griffith, Vol. 33 of Bulletin of the American Astronomical Society, 2001, p. 1079.

[7] R. Hu, S. Seager, Astrophys. J. 784 (1) (2014) 63. doi:10.1088/0004-637X/784/1/63.

[8] L. S. Rothman, I. E. Gordon, Y. Babikov, A. Barbe, D. C. Benner, P. F. Bernath, Others, J. Quant. Spectrosc. Radiat. Transfer 130 (0) (2013) 4–50. doi:10.1016/j.jqsrt.2013.07.002.

[9] Y. A. Ba, C. Wenger, R. Stotoeau, V. Boudon, M. Rotger, L. Daumont, D. A. Bonhommeau, V. G. Tyuterev, M.-L. Dubernet, J. Quant. Spectrosc. Radiat. Transfer 130 (SI) (2013) 62–68. doi:10.1016/j.jqsrt.2013.05.001.

[10] D. W. Schwenke, H. Partridge, J. Chem. Phys. 113 (16) (2000) 6592–6597. doi:http://dx.doi.org/10.1063/1.1311392.

[11] S. Yurchenko, J. Zheng, H. Lin, P. Jensen, W. Thiel, J. Chem. Phys. 123 (13) (2005) 134308.

[12] J. M. Bowman, T. Carrington, H.-D. Meyer, Mol. Phys. 106 (16-18) (2008) 2145–2182. doi:10.1080/00268970802258609.

[13] X. Huang, D. W. Schwenke, T. J. Lee, J. Phys. Chem. A 113 (43) (2009) 11954.

[14] X. Huang, D. W. Schwenke, T. J. Lee, J. Chem. Phys. 134 (4) (2011) 044320.

[15] L. Lodi, J. Tennyson, J. Quant. Spectrosc. Radiat. Transfer 113 (11) (2012) 850 – 858. doi:10.1016/j.jqsrt.2012.02.023.

[16] M. Rey, A. V. Nikitin, V. G. Tyuterev, Phys. Chem. Chem. Phys. 15 (25) (2013) 10049–10061. doi:10.1039/c3cp50275a.

[17] V. G. Tyuterev, R. V. Kochanov, S. A. Tashkun, F. Holka, P. G. Szalay, J. Chem. Phys. 139 (13) (2013) 134307.

[18] A. V. Nikitin, M. Rey, V. G. Tyuterev, Chem. Phys. Lett. 565 (2013) 5–11. doi:10.1016/j.cplett.2013.02.022.

[19] A. Nikitin, M. Rey, V. G. Tyuterev, J. Mol. Spectrosc. 305 (0) (2014) 40 – 47. doi:10.1016/j.jms.2014.09.010.

[20] N. F. Zobov, S. V. Shirin, R. I. Ovsyannikov, O. L. Polyansky, R. J. Barber, J. Tennyson, P. F. Bernath, M. Carleer, R. Colin, P.-F. Coheur, Mon. Not.

R. Astron. Soc. 387 (3) (2008) 1093–1098. doi:10.1111/j.1365-2966.2008.13234.x.

[21] A. Campargue, A. Barbe, M.-R. De Backer-Barilly, V. G. Tyuterev, S. Kassi, Phys. Chem. Chem. Phys. 10 (2008) 2925–2946. doi:10.1039/B719773J.

[22] V. G. Tyuterev, S. Tashkun, M. Rey, R. Kochanov, A. Nikitin, T. Delahaye, J. Phys. Chem. A 117 (50) (2013) 13779. doi:10.1021/jp408116j.

[23] V. G. Tyuterev, R. Kochanov, A. Campargue, S. Kassi, D. Mondelain, A. Barbe, E. Starikova, M. R. De Backer, P. G. Szalay, S. Tashkun, Phys. Rev. Lett. 113 (2014) 143002. doi:10.1103/PhysRevLett.113.143002.

[24] M. Rey, A. V. Nikitin, V. G. Tyuterev, J. Chem. Phys. 141 (4) (2014) 044316. doi:10.1063/1.4890956.

[25] M. Rey, A. V. Nikitin, V. G. Tyuterev, J. Quant. Spectrosc. Radiat. Transfer 164 (2015) 207 – 220. doi:10.1016/j.jqsrt.2015.06.009.

[26] M. Rey, A. V. Nikitin, V. G. Tyuterev, Astrophys. J. 789 (1) (2014) 2. doi:10.1088/0004-637X/789/1/2.

[27] S. N. Yurchenko, J. Tennyson, Mon. Not. R. Astron. Soc. 440 (2) (2014) 1649–1661. arXiv:http://mnras.oxfordjournals.org/content/440/2/1649.full.pdf+html, doi:10.1093/mnras/stu326.

[28] M. Rotger, V. Boudon, J. V. Auwera, J. Quant. Spectrosc. Radiat. Transfer 109 (6) (2008) 952–962. doi:10.1016/j.jqsrt.2007.12.005.

[29] M. A. Loroño Gonzalez, V. Boudon, M. Loëte, M. Rotger, M. T. Bourgeois, K. Didriche, M. Herman, V. A. Kapitanov, Y. N. Ponomarev, A. A. Solodov, A. M. Solodov, T. M. Petrova, J. Quant. Spectrosc. Radiat. Transfer 111 (15, SI) (2010) 2265–2278. doi:10.1016/j.jqsrt.2010.04.010.

[30] O. N. Ulenikov, G. A. Onopenko, E. S. Bekhtereva, T. M. Petrova, A. M. Solodov, A. A. Solodov, Mol. Phys. 108 (5) (2010) 637–647. doi:10.1080/00268971003645362.

[31] A. Ben Hassen, F. K. Tchana, J. M. Flaud, W. J. Lafferty, X. Landsheere, H. Aroui, J. Mol. Spectrosc. 282 (2012) 30–33. doi:10.1016/j.jms.2012.11.001.

[32] O. N. Ulenikov, O. V. Gromova, Y. S. Aslapovskaya, V. M. Horneman, J. Quant. Spectrosc. Radiat. Transfer 118 (2013) 14–25. doi:10.1016/j.jqsrt.2012.11.032.

[33] M.-T. Bourgeois, A. Alkadrou, M. Rotger, J. Vander Auwera, V. Boudon, to be submitted...

[34] S. Carter, A. R. Sharma, J. M. Bowman, J. Chem. Phys. 137 (15). doi:10.1063/1.4758005.

[35] P. Cassam-Chenai, J. Lievin, J. Chem. Phys. 136 (17). doi:10.1063/1.4705278.

[36] J. M. L. Martin, T. J. Lee, P. R. Taylor, J. P. Francois, J. Chem. Phys. 103 (7) (1995) 2589–2602. doi:10.1063/1.469681.

[37] G. Avila, T. Carrington Jr., J. Chem. Phys. 135 (6). doi:10.1063/1.3617249.

[38] T. Delahaye, A. Nikitin, M. Rey, P. G. Szalay, V. G. Tyuterev, J. Chem. Phys. 141 (10) (2014) 104301. doi:10.1063/1.4894419.

[39] G. D. Purvis, R. J. Bartlett, J. Chem. Phys. 76 (4) (1982) 1910–1918. doi:10.1063/1.443164.

[40] K. Raghavachari, G. W. Trucks, M. Head-Gordon, J. A. Pople, Chem. Phys. Lett. 157 (1989) 479.

[41] T. H. Dunning, J. Chem. Phys. 90 (2) (1989) 1007–1023. doi:10.1063/1.456153.

[42] K. A. Peterson, T. B. Adler, H.-J. Werner, J. Chem. Phys. 128 (8) (2008) 084102. doi:10.1063/1.2831537.

[43] H. J. Werner, P. J. Knowles, G. Knizia, F. R. Manby, M. Schütz, Others (2012).

[44] D. W. Schwenke, J. Phys. Chem. A 105 (11) (2001) 2352–2360. doi:10.1021/jp0032513.

[45] J. K. G. Watson, Mol. Phys. 15 (5) (1968) 479–490. doi:10.1080/00268976800101381.

[46] G. B. Lebron, T. L. Tan, Int. J. Spectrosc. 2012 (2012) 474639. doi:10.1155/2012/474639.

[47] V. I. Perevalov, V. G. Tyuterev, B. I. Zhilinskii, J. Phys. Paris 43 (5) (1982) 723–728.

[48] V. I. Perevalov, V. G. Tyuterev, B. I. Zhilinskii, Chem. Phys. Lett. 104 (5) (1984) 455–461.

[49] V. G. Tyuterev, J. P. Champion, G. Pierre, V. I. Perevalov, J. Mol. Spectrosc. 120 (1) (1986) 49–78.